



# Usefulness of [<sup>18</sup>F]fluorodeoxyglucose PET/CT for evaluating the PD-L1 status in nasopharyngeal carcinoma

Liang Zhao<sup>1</sup> · Yanzhen Zhuang<sup>2</sup> · Kaili Fu<sup>1</sup> · Peiqiong Chen<sup>2</sup> · Yuhuan Wang<sup>2</sup> · Jianfang Zhuo<sup>1</sup> · Xiyi Liao<sup>1</sup> · Haojun Chen<sup>3</sup> · Qin Lin<sup>1</sup>

Received: 12 October 2019 / Accepted: 9 December 2019 / Published online: 3 January 2020  
© Springer-Verlag GmbH Germany, part of Springer Nature 2020

## Abstract

**Purpose** To explore the relationship between [<sup>18</sup>F]fluorodeoxyglucose (<sup>18</sup>F-FDG uptake) and PD-L1 expression and determine the usefulness of <sup>18</sup>F-FDG PET/CT for evaluating the PD-L1 status in tumour cells (TCs) and tumour-infiltrating immune cells (TIICs) in patients with nasopharyngeal carcinoma (NPC).

**Methods** We retrospectively evaluated the records of 84 eligible patients who received an initial histopathological diagnosis of NPC between December 2016 and March 2019. All tissue specimens and PET/CT images were collected prior to treatment. High PD-L1 expression in TCs and TIICs was defined as ≥ 50% of stained cells.

**Results** There was a significant difference in <sup>18</sup>F-FDG uptake according to the PD-L1 status in TCs and TIICs. Univariate analysis showed that PD-L1 expression in TCs was associated with tumour maximum standardized uptake value (SUVmax) ( $P < 0.001$ ), primary tumour total lesion glycolysis (TLG;  $P < 0.001$ ), and T stage ( $P = 0.044$ ), but not with plasma Epstein-Barr virus (EBV) load ( $P = 0.816$ ), whereas PD-L1 expression in TIICs was related to SUVmax ( $P = 0.011$ ), TLG ( $P = 0.001$ ), T stage ( $P = 0.028$ ), and plasma EBV load ( $P = 0.003$ ). In multivariate logistic regression, PD-L1 expression in TCs was positively associated with SUVmax ( $P = 0.003$ ) and TLG ( $P = 0.001$ ), and in TIICs, negatively associated with SUVmax ( $P = 0.038$ ) and plasma EBV load ( $P = 0.025$ ).

**Conclusions** <sup>18</sup>F-FDG uptake in NPC lesions was positively correlated with PD-L1 expression in TCs and negatively correlated with PD-L1 expression in TIICs. Thus, <sup>18</sup>F-FDG PET/CT may be useful for evaluating the PD-L1 status in patients with NPC.

**Keywords** Nasopharyngeal carcinoma · PD-L1 · PET/CT · SUVmax · TLG

---

Liang Zhao, Yanzhen Zhuang and Kaili Fu contributed equally to this work.

---

This article is part of the Topical Collection on Oncology – Head and Neck.

---

**Electronic supplementary material** The online version of this article (<https://doi.org/10.1007/s00259-019-04654-4>) contains supplementary material, which is available to authorized users.

---

✉ Haojun Chen  
leochen0821@foxmail.com

✉ Qin Lin  
linqin05@163.com

<sup>1</sup> Department of Radiation Oncology, Xiamen Cancer Hospital, The First Affiliated Hospital of Xiamen University, Teaching Hospital of Fujian Medical University, Xiamen, China

<sup>2</sup> Department of Pathology, The First Affiliated Hospital of Xiamen University, Teaching Hospital of Fujian Medical University, Xiamen, China

<sup>3</sup> Department of Nuclear Medicine & Minnan PET Center, Xiamen Cancer Hospital, The First Affiliated Hospital of Xiamen University, Teaching Hospital of Fujian Medical University, Xiamen, China

## Introduction

Nasopharyngeal carcinoma (NPC), a malignant cancer arising from the nasopharynx epithelium, has a distinct geographical distribution in North Africa and parts of Asia [1, 2]. In these endemic areas, the main histological subtypes are predominantly associated with Epstein-Barr virus (EBV) infection [1, 3]. NPC is sensitive to chemotherapy and radiotherapy, and the 5-year overall survival of early-stage NPC has risen to more than 90% [4]. However, the clinical outcome of recurrent and distant metastatic NPC with conventional therapy remains disappointing [5]. GLOBOCAN 2018 estimates that the worldwide mortality rate for NPC is over 70,000 cases per year [6].

Immune checkpoint blockades (ICBs), especially PD-1/PD-L1 blockades, which harness the power of the hosts' immune system to cure cancer, have changed the landscape of advanced tumour therapy in recent years [7]. PD-1/PD-L1 blockades have greatly improved the outcomes in various tumour types, such as non-small-cell lung cancer (NSCLC), melanoma, and head and neck squamous cell carcinoma (HNSCC) [8–10]. Since NPC is closely associated with EBV infection, the immune cells can more easily infiltrate the tumour regions in patients with NPC. Thus, immunotherapy may also be appropriate for the treatment of NPC. Indeed, three phase I–II clinical trials have shown promising antitumour activity and safety in PD-1/PD-L1 blockades for advanced NPC [11–13]. In the Mayo Clinic Phase 2 study (NCI-9742), a descriptive analysis showed that patients with NPC with PD-L1-positive tumours showed a higher proportion response rate to PD-1 blockades [13]. In another study that investigated the therapeutic efficacy of pembrolizumab versus standard chemotherapy for recurrent or metastatic head and neck squamous cell carcinoma (Keynote 040), in a population with tumour cell (TC) PD-L1 expression in proportion  $\geq 50\%$ , the pembrolizumab group had better overall survival (OS) than did the standard-of-care group [14]. Moreover, a phase 3 study of first-line pembrolizumab for recurrent/metastatic head and neck squamous cell carcinoma (Keynote 048) showed that PD-L1 expression in TCs and tumour-infiltrating immune cells (TIICs) could predict the therapeutic efficacy of pembrolizumab [15]. In the groups with PD-L1 combined positive score (CPS) either  $\geq 20$  or  $\geq 1$ , pembrolizumab monotherapy or in combination with chemotherapy led to significant improvement in OS compared with the groups treated with first-line conventional therapy [15]. Based on this study, the FDA designated pembrolizumab for the first-line treatment of recurrent or metastatic HNSCC in patients whose tumours express PD-L1 (CPS  $\geq 1$ ) on June 2019. Although the predictive value of PD-L1 expression in NPC remains controversial, the PD-L1 status is still a stratification factor for ongoing clinical trials on NPC, such as NCT03558191, NCT03581786, and NCT03707509. Thus,

PD-L1 expression in TCs and TIICs remains valuable for NPC study.

[ $^{18}\text{F}$ ]Fluorodeoxyglucose ( $^{18}\text{F}$ -FDG) positron emission tomography (PET) is an important molecular imaging modality that is used for diagnosing NPC and performing TNM staging in patients with NPC [16]. The maximum standardized uptake value (SUVmax) on  $^{18}\text{F}$ -FDG-PET, which reflects FDG uptake in tumour lesions, is widely used in clinical practice due to its simplicity. Total lesion glycolysis (TLG), also known as the total glycolytic burden of disease, could effectively reflect tumour vitality and burden from the baseline  $^{18}\text{F}$ -FDG PET/computed tomography (CT) scans. A high SUVmax or TLG value has been reported to be an important prognostic factor in a variety of malignancies, including NPC [17, 18]. Some studies have reported a correlation between FDG uptake and tumour biomarker levels in different types of cancer, such as HER2 expression in gastric cancer [19] and EGFR expression in breast cancer and NSCLC [20, 21]. Similarly, other studies have shown PD-L1 expression to be correlated with FDG uptake in bladder cancer and NSCLC [22, 23]. Therefore, evaluation of  $^{18}\text{F}$ -FDG uptake patterns may be a useful method for non-invasively inferring the PD-L1 status in patients with NPC.

Therefore, the aim of the present study was to explore the relationship between  $^{18}\text{F}$ -FDG uptake and PD-L1 expression and determine the usefulness of  $^{18}\text{F}$ -FDG PET/CT for evaluating the PD-L1 status in TCs and TIICs in patients with NPC. Studies focused on  $^{18}\text{F}$ -FDG PET/CT parameters, and the PD-L1 status in NPC is rare, and our data may provide valuable information that can help in making decisions regarding PD-1/PD-L1 blockade therapy for patients with NPC.

## Materials and methods

### Study population

This retrospective study was approved by the Clinical Research Ethics Committee of the First Affiliated Hospital of Xiamen University (KY2017–015) and conducted in accordance with the 1964 Declaration of Helsinki and its later amendments or comparable ethical standards. The study group comprised 84 patients who received an initial histopathological diagnosis of NPC between December 2016 and March 2019 at the First Affiliated Hospital of Xiamen University. The inclusion criteria were as follows: (i) pathologically confirmed non-keratinizing differentiated or undifferentiated carcinoma (WHO classes II and III), (ii) whole-body  $^{18}\text{F}$ -FDG PET/CT performed at our institution within 3 weeks of pathological confirmation, (iii) collection of all tissue specimens and  $^{18}\text{F}$ -FDG PET/CT images and evaluation of the plasma EBV-DNA load before any treatments, and (iv) availability of complete clinical records, including data on

age, sex, smoking history, and nasopharyngeal magnetic resonance imaging. The exclusion criteria were as follows: (i) history of adjuvant therapy before  $^{18}\text{F}$ -FDG PET/CT imaging and (ii) incomplete clinical and pathological data. Among the 188 patients with NPC for whom immunohistochemical (IHC) staining for PD-L1 was performed during this period, only 84 met the inclusion and exclusion criteria. The EBV-

DNA load in plasma was analysed by polymerase chain reaction. The clinical stage was determined by a physician according to the eighth edition of the American Joint Committee on Cancer staging of NPC. Tissue samples were obtained from the patients after they provided written informed consent.

### Characteristics of the patients

**Table 1** Clinical characteristics of the study patients

Variable	Number	%
Age (years)		
< 49	41	48.8%
≥ 49	43	51.2%
Range	20–72	
Median	49	
Mean ± SD	47 ± 11	
Sex		
Male	55	65.5%
Female	29	34.5%
Histology, WHO type		
II	5	6.0%
III	79	94.0%
Smoking history		
Non-smoker	43	51.2%
Smoker	41	48.8%
T stage		
T1/T2	38	45.2%
T3/T4	46	54.8%
N stage		
N0–N2	56	66.7%
N3	28	33.3%
M stage		
M0	76	90.5%
M1	8	9.5%
Clinical stage		
I/II/III	44	52.4%
IVa/b	40	47.6%
Plasma EBV-DNA load (IU/ml)		
< 50	23	27.4%
≥ 50	61	72.6%
PD-L1 expression in TCs (%)		
< 50	24	28.6%
≥ 50	60	71.4%
PD-L1 expression in TIICs (%)		
< 50	71	84.5%
≥ 50	13	15.5%
SUVmax		
Mean ± SD	9.3 ± 4.1	
TLG		
Mean ± SD	64.8 ± 58.5	

IHC staining for PD-L1 expression was performed for all 188 patients with NPC. Among these, 131 showed high PD-L1 expression in TCs (69.7%), and 25 (13.3%) showed high PD-L1 expression in TIICs (Supplemental Table 1). The clinical characteristics of the 84 enrolled patients are summarized in Table 1 and Supplemental Table 2. The median age of the patients was 49 years (range: 20–72 years). Forty-one (48.8%) patients were current or former smokers. Disease in stages I–III accounted for 44 (52.4%) cases, while stage IVa–b was identified in 40 (47.6%) cases. The SUVmax in PET/CT imaging of the primary tumours ranged from 3.1 to 21.4, with a median value of 8.4. High PD-L1 expression in TCs was confirmed in 60 (71.4%) cases, while only 13 (15.5%) patients exhibited high PD-L1 expression in TIICs. Although the proportion of high/low PD-L1 expression in TCs or TIICs was not near equal, the proportion of PD-L1 expression in the 84 enrolled patients was similar to that in all 188 patients. As such, the imbalance in PD-L1 expression could be considered an objective phenomenon and would not bias the final results.

### Immunohistochemistry

Formalin-fixed, paraffin-embedded tumour tissues were sectioned at 4- $\mu\text{m}$  thickness. For IHC detection of PD-L1, we used the BenchMark GX automated slide stainer (SP263, Ventana, Oro Valley, AZ, USA) to stain the sections with the PD-L1 antibody according to the manufacturer's recommended protocol. Positive control (placenta) and negative control samples were run simultaneously with each specimen.

The immunostained tissue sections were scored by two independent investigators who were blinded to the clinical data. High PD-L1 expression in TCs or TIICs was defined as  $\geq 50\%$  of corresponding cells with membranous staining as described by a previous study [24].

### $^{18}\text{F}$ -FDG PET/CT protocol and imaging analysis

All patients were required to fast for at least 6 h prior to the examination.  $^{18}\text{F}$ -FDG was manufactured in accordance with the standard method described by our laboratory, using the coincidence  $^{18}\text{F}$ -FDG synthesis module (TracerLab FxFN, GE Healthcare). Quality control of the radiosynthesis was performed by ultraviolet and radio-high-performance liquid chromatography (HPLC). The radiochemical purity was over 98%, and the final product was diluted with saline and

sterilized by passing it through a 0.22- $\mu\text{m}$  Millipore filter into a sterile syringe. The dose of intravenously injected  $^{18}\text{F}$ -FDG was calculated according to the patient's weight (3.7 MBq [0.1 mCi]/kg). Data were acquired using a PET/CT system (Discovery ST; GE Medical Systems, Waukesha, WI, USA) after 1 h of intravenous administration. The parameters for the acquisition were as follows: CT scanning included the area from the head to the upper thighs. A PET scan was performed immediately after CT acquisition with 1.5 min of scanning time per table position, with the acquisition in 3-D mode. All the obtained data were transferred to the Advantage Workstation (Version AW 4.6, GE Healthcare, Waukesha, WI, USA); data were reconstructed using the ordered subset expectation maximization algorithm (2 iterations and 21 subsets), using CT data for attenuation correction, and the reconstructed images were then co-registered and displayed.

### PET/CT imaging analysis

Fused PET/CT images were viewed on the Advantage Workstation (Version AW 4.6, GE Healthcare). Regions of interest were drawn on transaxial images around the primary tumours for the purpose of semiquantitative analysis. The SUVmax and SUVmean values were automatically calculated and were used to quantify the uptake of FDG in primary tumours. For delineation of the metabolic tumour volume (MTV), PET images were reviewed with an SUV intensity range of 0–5 for localization of the hypermetabolic lesion in the nasopharynx, and boundaries that were large enough were drawn to include the hypermetabolic lesion in the axial, coronal, and sagittal  $^{18}\text{F}$ -FDG PET/CT images. Then, an isocontour connecting the lesion showing an SUV of 2.5 was set automatically inside the boundary, and all voxels with an SUV of 2.5 or greater within the isocontour line were counted for the calculation of the MTV. The MTV was defined as the sum of voxels that showed an SUV of 2.5 or higher. TLG for the primary tumours was calculated as the sum of the product of the SUVmean and MTV of the primary tumours (TLG = sum of [SUVmean  $\times$  MTV]).

### Statistical analysis

All statistical analyses were conducted using the SPSS 22.0 statistical analysis software (IBM, Armonk, NY, USA). Receiver-operating characteristic (ROC) curves were used for the FDG-PET parameters to generate the optimal cut-off values of PD-L1 expression [25]. For categorical variables, either the chi-squared test, Yates' correction of chi-squared test, or Fisher's exact test was used to analyse the differences between groups. For continuous data, we used the t-test or the Wilcoxon test for analyses, as appropriate. Factors identified as significantly associated with PD-L1 expression after univariate analysis were subsequently entered into the

multivariable analyses via a logistic regression model. All tests were two-sided, and a *P* value lower than 0.05 was considered statistically significant.

## Results

### Association between $^{18}\text{F}$ -FDG uptake and PD-L1 expression in TCs and TIICs

The comparison of  $^{18}\text{F}$ -FDG uptake based on PD-L1 expression in TCs and TIICs revealed a significant difference (Fig. 1). In TCs, the values of SUVmax in patients with high PD-L1 expression were significantly higher than those in patients with low PD-L1 expression (SUVmax:  $10.2 \pm 4.1$  vs.  $6.9 \pm 3.2$ ;  $P < 0.001$ ), whereas, in TIICs, the accumulation of  $^{18}\text{F}$ -FDG was lower in patients with high PD-L1 expression than in those with low expression (SUVmax:  $7.0 \pm 3.4$  vs.  $9.7 \pm 4.1$ ;  $P = 0.008$ ). This phenomenon was also observed in the TLG values for high and low PD-L1 expression in TCs (TLG:  $76.7 \pm 64.4$  vs.  $35.0 \pm 20.5$ ;  $P < 0.001$ ) and in TIICs (TLG:  $29.1 \pm 14.4$  vs.  $71.3 \pm 61.2$ ;  $P = 0.001$ ), respectively. Typical thin-section CT and PET/CT and IHC staining images of PD-L1 with high and low expression are shown in Fig. 2.

We plotted a ROC curve to calculate the most discriminative cut-off value of SUVmax and TLG for determining positive PD-L1 expression in TCs and TIICs. Regarding PD-L1 expression in TCs, the optimal cut-off values for SUVmax and TLG were 6.7 (area under curve (AUC) value = 0.762;  $P < 0.001$ ) and 41.3 (AUC value = 0.756;  $P < 0.001$ ), respectively (Supplemental Fig. 1a, b). With respect to PD-L1 expression in TIICs, the optimal cut-off values for SUVmax and TLG were 7.2 (AUC value = 0.733;  $P = 0.008$ ) and 53.0 (AUC value = 0.785;  $P = 0.001$ ), respectively (Supplemental Fig. 1c, d).

### Correlations between patient characteristics and PD-L1 expression in TCs and TIICs

We examined the correlation between patient characteristics (including SUVmax and TLG) and PD-L1 expression in TCs and TIICs. Among the 84 patients, 71.4% showed high PD-L1 expression in TCs, while 15.5% showed high PD-L1 expression in TIICs.

Univariate analysis showed that expression of PD-L1 in TCs was associated with SUVmax ( $P = 0.001$ ) and T stage ( $P = 0.034$ ) but not with MTV ( $P = 0.298$ ) and plasma EBV load ( $P = 0.216$ ; Table 2). PD-L1 expression in TIICs was related to SUVmax ( $P < 0.001$ ), T stage ( $P = 0.004$ ), and plasma EBV load ( $P = 0.032$ ), but not to MTV ( $P = 0.100$ ; Table 2).

In multivariate logistic regression analysis, PD-L1 expression in TCs was significantly associated with SUVmax ( $P = 0.001$ ) and TLG ( $P = 0.006$ ), but not with T stage ( $P = 0.754$ ); PD-L1 expression in TIICs was associated with SUVmax

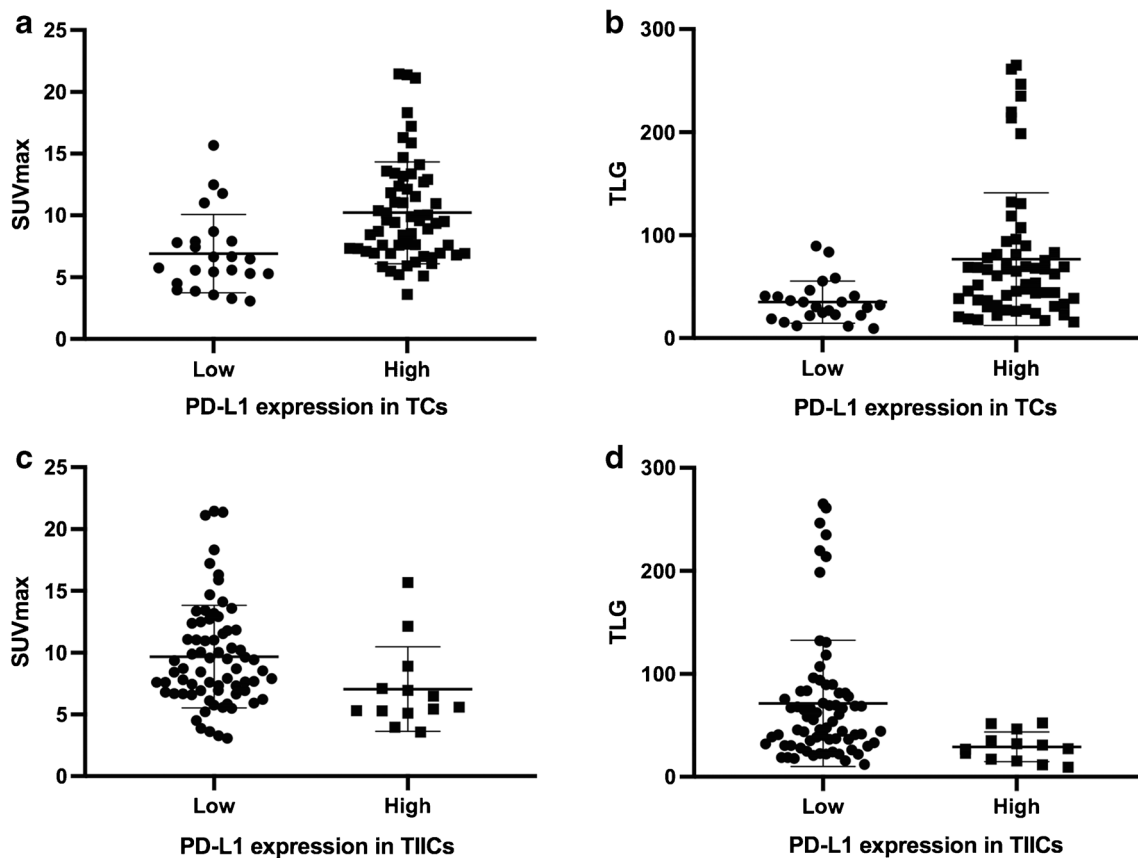


**Fig. 1** Relationship between  $^{18}\text{F}$ -FDG uptake and PD-L1 expression in patients with NPC. (a) Correlation between SUVmax and PD-L1 expression in TCs. SUVmax was significantly higher in tumours with high PD-L1 expression than in those with low PD-L1 expression (SUVmax:  $10.2 \pm 4.1$  vs.  $6.9 \pm 3.2$ ;  $P < 0.001$ ). (b) Correlation between primary tumour TLG and PD-L1 expression in TCs. TLG was significantly higher in tumours with high PD-L1 expression than in those with low PD-L1 expression (TLG:  $76.7 \pm 64.4$  vs.  $35.0 \pm 20.5$ ;  $P < 0.001$ ). (c) Correlation between SUVmax and PD-L1 expression in TIICs. SUVmax was significantly lower in tumours with high PD-L1 than in those with low PD-L1 expression (SUVmax:  $7.0 \pm 3.4$  vs.  $9.7 \pm 4.1$ ;  $P = 0.011$ ). (d) Correlation between primary tumour TLG and PD-L1 expression in TIICs. TLG was significantly lower in tumours with high PD-L1 expression than in those with low PD-L1 expression (TLG:  $29.1 \pm 14.4$  vs.  $71.3 \pm 61.2$ ;  $P = 0.001$ )

$^{18}\text{F}$ -FDG  $^{18}\text{F}$ -Fluorodeoxyglucose, NPC nasopharyngeal carcinoma, SUVmax maximum standardized uptake value, TC tumour cell, TIIC tumour-infiltrating immune cell, TLG total lesion glycolysis

( $P = 0.038$ ) and plasma EBV load ( $P = 0.025$ ), but not with T stage ( $P = 0.384$ ) or TLG ( $P = 0.998$ ; Table 3). After determining that SUVmax and TLG were correlated with PD-L1 expression in TCs and that TLG was correlated with PD-L1 expression in TIICs, we used these PET/CT parameters separately to predict PD-L1 expression in TCs and TIICs. We determined that a SUVmax cut-off value of 6.7 and a TLG cut-off value of 41.3 obtained a maximum accuracy of 78.6% and 71.4%, respectively, for predicting PD-L1 expression in TCs. A SUVmax cut-off value of 7.2 obtained a maximum accuracy of 71.4% for predicting PD-L1 expression in TIICs.

Both SUVmax and TLG/plasma EBV-DNA load were independently associated with PD-L1 status in TCs/TIICs in the univariate and multivariate analyses; therefore, we analysed the combined effect of SUVmax and TLG/plasma EBV-DNA on the PD-L1 status of patients with NPC. All patients were divided into three groups based on SUVmax and TLG to assess the probability of PD-L1 status in TCs: a low-probability group (SUVmax  $< 6.7$  and TLG  $< 41.3$ ),

an intermediate-probability group (SUVmax  $\geq 6.7$  and TLG  $< 41.3$  or SUVmax  $< 6.7$  and TLG  $\geq 41.3$ ), and a high-probability group (SUVmax  $\geq 6.7$  and TLG  $\geq 41.3$ ). The probabilities of high PD-L1 status TCs in these groups were 25%, 67%, and 95%, respectively ( $P < 0.001$ ; Table 4). This result indicates that high SUVmax and TLG values predict high PD-L1 expression status in TCs. Similarly, patients were divided into three groups based on SUVmax and plasma EBV-DNA to assess the probability of PD-L1 status in TIICs: a low-probability group (SUVmax  $\geq 7.2$  and plasma EBV-DNA  $\geq 50$ ), an intermediate-probability group (SUVmax  $< 7.2$  and plasma EBV-DNA  $\geq 50$  or SUVmax  $\geq 7.2$  and plasma EBV-DNA  $< 50$ ), and a high-probability group (SUVmax  $< 7.2$  and plasma EBV-DNA  $< 50$ ). The probabilities of low PD-L1 status in TIICs in these groups were 98%, 82%, and 40%, respectively ( $P < 0.001$ ; Table 4), suggesting that a high SUVmax value and a high plasma EBV-DNA load predict low PD-L1 expression status in TIICs.

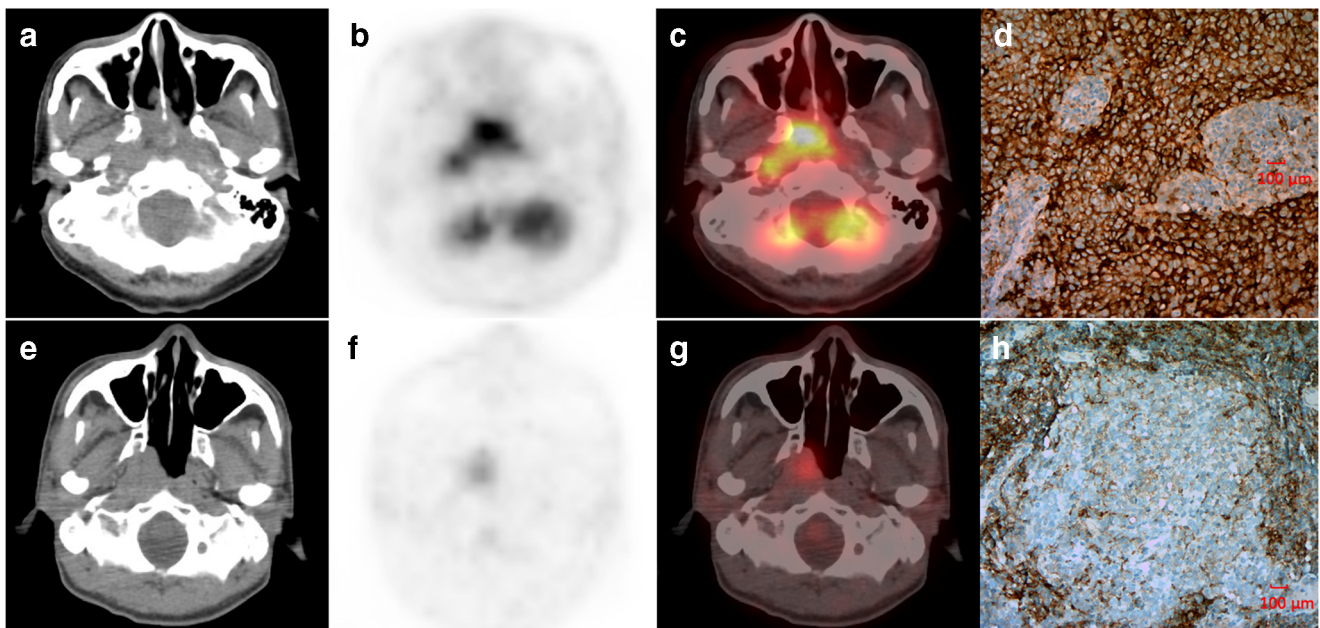


**Fig. 2** Representative images of CT (a, e),  $^{18}\text{F}$ -FDG PET (b, f), PET/CT (c, g), and immunohistochemistry of PD-L1 expression (d, h) in patients with NPC

Patient I (upper row) showed intense uptake in nasopharyngeal lesion ( $\text{SUV}_{\text{max}} = 10.0$ ,  $\text{TLG} = 89.7$ ), while the proportion of PD-L1 expression in TCs and TIICs was 90% and 10%, respectively (Fig. 2d). Patient II (lower row) showed lower increased activity in nasopharyngeal

lesion ( $\text{SUV}_{\text{max}} = 5.44$ ,  $\text{TLG} = 26.81$ ), while the proportion of PD-L1 expression in TCs and TIICs was 10% and 80%, respectively (Fig. 2h). *CT* computed tomography,  $^{18}\text{F}$ -FDG  $^{18}\text{F}$ -Fluorodeoxyglucose, *NPC* nasopharyngeal carcinoma, *PET/CT* positron emission tomography/computed tomography,  $\text{SUV}_{\text{max}}$  maximum standardized uptake value, *TC* tumour cell, *TIIC* tumour-infiltrating immune cell, *TLG* total lesion glycolysis

## Discussion

No other imaging modality has played such an important role in the field of immunotherapy as has molecular imaging. Many preclinical and initial clinical trials have explored the use of novel molecular imaging agents to map the in vivo distribution of immunotherapy-related biomarkers or target immune checkpoints, such as radiolabelled PD-1 and PD-L1 antibodies [26, 27]. However, these imaging agents are yet to be widely applied in clinical settings, and the relatively low density of biomarker expression complicates imaging interpretation. Therefore, more universal imaging tracers such as  $^{18}\text{F}$ -FDG are being tested in many immunotherapy settings. In the present study, we found a statistically significant correlation between FDG-PET parameters and PD-L1 expression in patients with NPC. Generally, primary tumour  $\text{SUV}_{\text{max}}$  and  $\text{TLG}$  were positively related to PD-L1 expression in TCs, while  $\text{SUV}_{\text{max}}$  and plasma EBV load were negatively associated with PD-L1 expression in TIICs. Previous studies have shown similar findings, i.e. that PD-L1 expression in TCs was correlated with  $\text{SUV}_{\text{max}}$  in lung cancer and bladder cancer [22, 23]. However, these studies did not analyse the correlation between primary tumour  $\text{TLG}$  and PD-L1 status, and they also did not sufficiently study PD-L1 expression in TIICs. Our results showed that  $^{18}\text{F}$ -FDG PET/CT could be potentially useful for evaluation of the PD-L1 status in patients with NPC.

However, the specific mechanism behind the correlation between  $^{18}\text{F}$ -FDG uptake and PD-L1 expression is unknown. It should be noted that although a high tumour stage independently correlates with increased tracer accumulation, other factors could be at play in addition to the expression of PD-L1. There is growing evidence that tumour metabolism plays an important role in the antitumour immune pathway [28]. An elevated FDG uptake is usually associated with the expression of phosphorylated STAT3 (pSTAT3), GLUT1, and the hypoxia-inducible factor-1 $\alpha$  (HIF-1 $\alpha$ ) [29], which represent high TC proliferation, glucose metabolism, and hypoxia, respectively [30]. In patients with EBV-positive NPC, latent membrane protein 1 (LMP1) of the EBV has been reported to increase PD-L1 expression in TCs with a concomitant increase of pSTAT3, while blocking pSTAT3 reduces LMP1-induced PD-L1 expression [31]. These findings indicate that the positive association between FDG uptake and PD-L1 expression in TCs may reflect the activation of the pSTAT3 pathway. In addition, HIF-1 $\alpha$  has been reported to mediate intra-tumoural hypoxia and could be implicated in the upregulation of PD-L1 expression in malignant cell downregulation of T cell function [32]. Previous clinical studies have shown that both primary tumour  $\text{SUV}_{\text{max}}$  and  $\text{TLG}$  predicted unfavourable clinical outcome [17, 18] and that PD-L1 expression in TCs was also a negative indicator in NPC [33]. Taken together, primary tumour  $\text{SUV}_{\text{max}}$  and  $\text{TLG}$  may share a signalling pathway with PD-

**Table 2** Univariate analysis of the relationship between PD-L1 expression in TC and TIIC with disease variables

Variable	PD-L1 expression in TCs			PD-L1 expression in TIICs		
	Low	High	<i>P</i> value	Low	High	<i>P</i> value
Age (years)			0.403			0.900
49 (20–72)						
Gender			0.885			1.000
Male	16	39		46	9	
Female	8	21		25	4	
Histology, WHO type			0.942			1.000
II	2	3		4	1	
III	22	57		67	12	
Smoking history			0.890			0.693
Non-smoker	12	31		37	6	
Smoker	12	29		34	7	
T stage			0.044*			0.028*
T1/T2	15	23		28	10	
T3/T4	9	37		43	3	
N stage			0.608			0.594
N0-N2	17	39		46	10	
N3	7	21		25	3	
M stage			1.000			0.206
M0	22	54		63	13	
M1	2	6		8	0	
Clinical stage			0.240			0.104
I/II/III	15	29		34	10	
IVa/b	9	31		37	3	
Plasma EBV-DNA load (IU/ml)			0.816			0.003*
< 50	7	16		15	8	
≥ 50	17	44		56	5	
SUVmax			< 0.001*			0.003*
< 6.7	15	9		< 7.2	21	10
≥ 6.7	9	51		≥ 7.2	50	3
TLG			< 0.001*			0.001*
< 41.3	19	19		< 53.0	35	13
≥ 41.3	5	41		≥ 53.0	36	0

\*  $P < 0.05$ 

L1 expression in TCs, and, hence, all these three factors are related to adverse clinical outcome in patients with NPC. However, to truly understand the power of the  $^{18}\text{F}$ -FDG correlation with checkpoint expression, a large number of patients need to be followed to determine if the increased FDG uptake truly indicates higher checkpoint expression.

PD-L1 expression in TCs has been explored as a biomarker since the early stages of the development of PD-1/PD-L1 blockades, and it remains under debate whether we should stain only TCs or both TCs and TIICs. Recently, there have been a growing number of clinical trials on PD-1/PD-L1 blockades focusing on PD-L1 expression in TCs and TIICs, both of which may be able to predict immune therapeutic

efficacy [15, 34]. PD-L1 expression in TIICs can be upregulated by exogenous inflammation-mediated immune responses within the intra-tumoural micro-environment, which indicates pre-existing immunity [35]. Thus, PD-L1 expression in TIICs is more strongly associated with the cancer immune response compared to that in TCs and has been proven as a favourable prognostic factor in various cancers [36]. In contrast, elevated SUVmax in patients with NPC predicts poor clinical outcome [1, 17, 37]. Enhanced glucose uptake by TCs deprives T cells of glucose and thus reduces the density of active T cells [28, 38]. This partly explains the negative association between SUVmax and PD-L1 expression in TIICs. However, the specific mechanism underlying this negative

**Table 3** Multivariate logistic regression analysis of the relationship between PD-L1 expression in TCs and TIICs with disease variables

	Factors	OR	95%CI	P value
PD-L1 expression in TCs	T stage	0.80	0.20–3.19	0.754
	SUVmax	7.81	2.38–25.61	0.001*
	TLG	7.56	1.77–32.32	0.006*
PD-L1 expression in TIICs	T stage	2.16	0.38–12.24	0.384
	Plasma EBV-DNA	5.87	1.25–21.49	0.025*
	SUVmax	5.41	1.10–26.72	0.038*
	TLG	0	0.00-	0.998

\* $P < 0.05$ 

association remains unknown and requires verification and further investigation.

As a way of determining the probability of TCs PD-L1 status, we divided our cohort into three groups based on both SUVmax and TLG; 95% of the patients in the high-probability group and 25% of the patients in the low-probability group had high PD-L1 expression in TCs. Regarding the probability of PD-L1 status in TIICs, the patients were also categorized based on both SUVmax and plasma EBV load. A similar trend was observed where 60% of the patients in the high-probability group and a mere 2% of those in the low-probability group had a high PD-L1 expression status. These results may be of significance for patients who would like to receive PD-1/PD-L1 blockades but are unable or unwilling to undergo biopsy for PD-L1 status testing.

Compared to previous studies that investigated the correlation between PD-L1 expression and FDG uptake, our study has the following advantages. First, we used PD-L1 antibodies that were examined in the Blueprint PD-L1 IHC Assay Comparison Project, which had a similar analytical presentation in terms of PD-L1 expression [39]. Second, the tumour specimens in our cohort were subjected to PD-L1 IHC staining immediately after nasopharyngoscopic biopsy. It has been shown that more accurate results are obtained using fresh tissue samples than using archived samples by avoiding antigen alterations or loss caused by long-term storage [40, 41]. More recently, there is some evidence that

temporal heterogeneity is observed in PD-L1 expression. In the 2019 ASCO meeting, it was reported that PD-L1 expression was significantly higher in fresh tissues (PD-L1 staining at < 90 days after biopsy) than in archival tissues (PD-L1 staining at > 90 days after biopsy) [42]. Moreover,  $^{18}\text{F}$ -FDG PET scanning of each patient was conducted within less than 3 weeks of biopsy. Such enrolment criteria may guarantee robust results regarding the correlation between FDG and PD-L1 expression.

Despite these strengths, our study has some notable limitations. First, this was a retrospective, single-centre study with a limited number of patients; therefore, a future multicentred study with a larger patient population should be conducted to determine the SUVmax and TLG cut-off values. Second, our cohort did not include patients who were treated with PD-1/PD-L1 blockades; therefore, it remains unclear whether  $^{18}\text{F}$ -FDG uptake can predict the response and prognosis of immunotherapy. Finally, even though  $^{18}\text{F}$ -FDG PET/CT may have moderate prediction performance, it cannot replace pathologic biopsy for examining PD-L1 status. Specifically, the mechanism underlying the high  $^{18}\text{F}$ -FDG uptake in PD-L1-positive tumours remains unclear. It should be noted that an advanced tumour stage independently correlates with increased tracer accumulation and factors other than the simple expression of PD-L1 could influence  $^{18}\text{F}$ -FDG uptake. As such, future immune PET with PD1/PD-L1-targeted agents may provide information complementing that obtained via  $^{18}\text{F}$ -FDG PET;

**Table 4** Combined factors to predict the probability of PD-L1 status in TCs and TIICs

	Probability	Number	PD-L1 status(%)		P value
			Low	High	
PD-L1 expression in TCs	Low	16	12 (75%)	4 (25%)	< 0.001
	Moderate	30	10 (33%)	20 (67%)	
	High	38	2 (5%)	36 (95%)	
PD-L1 expression in TIICs	Low	40	39 (98%)	1 (2%)	< 0.001
	Moderate	34	28 (82%)	6 (18%)	
	High	10	4 (40%)	6 (60%)	



such strategies could provide additional stratification information beyond that possible to obtain with  $^{18}\text{F}$ -FDG PET.

## Conclusion

$^{18}\text{F}$ -FDG uptake in NPC lesions was positively correlated with PD-L1 expression in TCs and negatively correlated with PD-L1 expression in TIICs. Therefore,  $^{18}\text{F}$ -FDG PET/CT imaging may be a useful alternative non-invasive strategy for predicting the PD-L1 status in patients with NPC, especially for those who cannot or are unwilling to undergo pathologic biopsy. Further prospective studies should validate this association.

**Funding information** This work was funded by the Natural Science Foundation of Fujian Province (Grant number 2016 J01633) and National Natural Science Foundation of China (Grant numbers 81772893 and 81701736).

## Compliance with ethical standards

**Conflict of interest** The authors declare that they have no conflict of interest.

**Ethical approval** All procedures performed in studies involving human participants were in accordance with the ethical standards of the institutional and/or national research committee and with the 1964 Helsinki Declaration and its later amendments or comparable ethical standards. This article does not contain any studies with animals performed by any of the authors.

**Informed consent** Informed consent was obtained from all individual participants included in the study.

## References

- Chua MLK, et al. Nasopharyngeal carcinoma. *Lancet*. 2016;387(10022):1012–24.
- Yu MC, Yuan JM. Epidemiology of nasopharyngeal carcinoma. *Semin Cancer Biol*. 2002;12(6):421–9.
- Chang ET, Adami HO. The enigmatic epidemiology of nasopharyngeal carcinoma. *Cancer Epidemiol Biomark Prev*. 2006;15(10):1765–77.
- Chen QY, et al. Concurrent chemoradiotherapy vs radiotherapy alone in stage II nasopharyngeal carcinoma: phase III randomized trial. *J Natl Cancer Inst*. 2011;103(23):1761–70.
- Lee AW, et al. Management of nasopharyngeal carcinoma: current practice and future perspective. *J Clin Oncol*. 2015;33(29):3356–64.
- Bray F, et al. Global cancer statistics 2018: GLOBOCAN estimates of incidence and mortality worldwide for 36 cancers in 185 countries. *CA Cancer J Clin*. 2018;68(6):394–424.
- Callahan MK, Postow MA, Wolchok JD. Targeting T cell co-receptors for cancer therapy. *Immunity*. 2016;44(5):1069–78.
- Larkins E, et al. FDA approval summary: pembrolizumab for the treatment of recurrent or metastatic head and neck squamous cell carcinoma with disease progression on or after platinum-containing chemotherapy. *Oncologist*. 2017;22(7):873–8.
- Ribas A, et al. Association of pembrolizumab with tumor response and survival among patients with advanced Melanoma. *JAMA*. 2016;315(15):1600–9.
- Borghaei H, et al. Nivolumab versus docetaxel in advanced nonsquamous non-small-cell lung cancer. *N Engl J Med*. 2015;373(17):1627–39.
- Fang W, et al. Camrelizumab (SHR-1210) alone or in combination with gemcitabine plus cisplatin for nasopharyngeal carcinoma: results from two single-arm, phase I trials. *Lancet Oncol*. 2018;19(10):1338–50.
- Hsu C, et al. Safety and antitumor activity of pembrolizumab in patients with programmed death-ligand 1-positive nasopharyngeal carcinoma: results of the KEYNOTE-028 Study. *J Clin Oncol*. 2017;JCO2017733675.
- Ma BBY, et al. Antitumor activity of nivolumab in recurrent and metastatic nasopharyngeal carcinoma: an international, multicenter study of the Mayo Clinic Phase 2 Consortium (NCI-9742). *J Clin Oncol*. 2018;36(14):1412–8.
- Cohen EEW, et al. Pembrolizumab versus methotrexate, docetaxel, or cetuximab for recurrent or metastatic head-and-neck squamous cell carcinoma (KEYNOTE-040): a randomised, open-label, phase 3 study. *Lancet*. 2019;393(10167):156–67.
- Saada-Bouzzid E, Peyrade F, Guigay J. Immunotherapy in recurrent and or metastatic squamous cell carcinoma of the head and neck. *Curr Opin Oncol*. 2019;31(3):146–51.
- Yen RF, et al. Early restaging whole-body ( $^{18}\text{F}$ )-FDG PET during induction chemotherapy predicts clinical outcome in patients with locoregionally advanced nasopharyngeal carcinoma. *Eur J Nucl Med Mol Imaging*. 2005;32(10):1152–9.
- Liu WS, et al. The role of pretreatment FDG-PET in nasopharyngeal carcinoma treated with intensity-modulated radiotherapy. *Int J Radiat Oncol Biol Phys*. 2012;82(2):561–6.
- Chang KP, et al. Prognostic significance of  $^{18}\text{F}$ -FDG PET parameters and plasma Epstein-Barr virus DNA load in patients with nasopharyngeal carcinoma. *J Nucl Med*. 2012;53(1):21–8.
- Chen R, et al. Relationship between  $^{18}\text{F}$ -FDG PET/CT findings and HER2 expression in gastric cancer. *J Nucl Med*. 2016;57(7):1040–4.
- Lee J, et al. Strong association of epidermal growth factor receptor status with breast cancer FDG uptake. *Eur J Nucl Med Mol Imaging*. 2017;44(9):1438–47.
- Lv Z, et al. Value of ( $^{18}\text{F}$ )-FDG PET/CT for predicting EGFR mutations and positive ALK expression in patients with non-small cell lung cancer: a retrospective analysis of 849 Chinese patients. *Eur J Nucl Med Mol Imaging*. 2018;45(5):735–50.
- Kaira K, et al. 2-Deoxy-2-[fluorine-18] fluoro-d-glucose uptake on positron emission tomography is associated with programmed death ligand-1 expression in patients with pulmonary adenocarcinoma. *Eur J Cancer*. 2018;101:181–90.
- Chen R, et al. Relationship between the expression of PD-1/PD-L1 and ( $^{18}\text{F}$ )-FDG uptake in bladder cancer. *Eur J Nucl Med Mol Imaging*. 2019;46(4):848–54.
- Zhao L, et al. Mismatch repair status and high expression of PD-L1 in nasopharyngeal carcinoma. *Cancer Manag Res*. 2019;11:1631–40.
- Takada K, et al. Metabolic characteristics of programmed cell death-ligand 1-expressing lung cancer on ( $^{18}\text{F}$ )-fluorodeoxyglucose positron emission tomography/computed tomography. *Cancer Med*. 2017;6(11):2552–61.
- Niemeijer AN, et al. Whole body PD-1 and PD-L1 positron emission tomography in patients with non-small-cell lung cancer. *Nat Commun*. 2018;9(1):4664.
- Hettich M, et al. High-resolution PET imaging with therapeutic antibody-based PD-1/PD-L1 checkpoint tracers. *Theranostics*. 2016;6(10):1629–40.

28. Chang CH, et al. Metabolic competition in the tumor microenvironment is a driver of cancer progression. *Cell*. 2015;162(6):1229–41.
29. Mano Y, et al. Correlation between biological marker expression and fluorine-18 fluorodeoxyglucose uptake in hepatocellular carcinoma. *Am J Clin Pathol*. 2014;142(3):391–7.
30. Doms C, et al. Association between 18F-fluoro-2-deoxy-D-glucose uptake values and tumor vitality: prognostic value of positron emission tomography in early-stage non-small cell lung cancer. *J Thorac Oncol*. 2009;4(7):822–8.
31. Fang W, et al. EBV-driven LMP1 and IFN-gamma up-regulate PD-L1 in nasopharyngeal carcinoma: implications for oncotargeted therapy. *Oncotarget*. 2014;5(23):12189–202.
32. Chen J, et al. Regulation of PD-L1: a novel role of pro-survival signalling in cancer. *Ann Oncol*. 2016;27(3):409–16.
33. Zhou Y, et al. PD-L1 predicts poor prognosis for nasopharyngeal carcinoma irrespective of PD-1 and EBV-DNA load. *Sci Rep*. 2017;7:43627.
34. Shitara K, et al. Pembrolizumab versus paclitaxel for previously treated, advanced gastric or gastro-oesophageal junction cancer (KEYNOTE-061): a randomised, open-label, controlled, phase 3 trial. *Lancet*. 2018;392(10142):123–33.
35. Pardoll DM. The blockade of immune checkpoints in cancer immunotherapy. *Nat Rev Cancer*. 2012;12(4):252–64.
36. Zhao T, et al. Prognostic value of PD-L1 expression in tumor infiltrating immune cells in cancers: a meta-analysis. *PLoS One*. 2017;12(4):e0176822.
37. Chan WK, et al. Prognostic impact of standardized uptake value of F-18 FDG PET/CT in nasopharyngeal carcinoma. *Clin Nucl Med*. 2011;36(11):1007–11.
38. Favaro E, et al. Glucose utilization via glycogen phosphorylase sustains proliferation and prevents premature senescence in cancer cells. *Cell Metab*. 2012;16(6):751–64.
39. Hirsch FR, et al. PD-L1 immunohistochemistry assays for lung cancer: results from phase 1 of the Blueprint PD-L1 IHC Assay Comparison Project. *J Thorac Oncol*. 2017;12(2):208–22.
40. Thompson RH, et al. Costimulatory molecule B7-H1 in primary and metastatic clear cell renal cell carcinoma. *Cancer*. 2005;104(10):2084–91.
41. Xie R, et al. Factors influencing the degradation of archival formalin-fixed paraffin-embedded tissue sections. *J Histochem Cytochem*. 2011;59(4):356–65.
42. Hong L, et al., Spatial and temporal heterogeneity of PD-L1 and its impact on benefit from immune checkpoint blockade in non-small cell lung cancer (NSCLC). *J Clin Oncol*, 2019. **suppl; abstr 9017**.

**Publisher's note** Springer Nature remains neutral with regard to jurisdictional claims in published maps and institutional affiliations.